JOURNAL OF AGRICULTURAL AND FOOD CHEMISTRY

Conformation of Napin (*Brassica juncea*) in Salts and Monohydric Alcohols: Contribution of Electrostatic and Hydrophobic Interactions

T. C. JYOTHI, SRIDEVI A. SINGH, AND A. G. APPU RAO*

Department of Protein Chemistry and Technology, Central Food Technological Research Institute, Mysore, India

Napin from mustard (*Brassica juncea* L.) is a seed storage protein consisting of two subunits linked through disulfide bonds and is predominantly helical in nature. Resistance to trypsin digestion and allergenicity limit its food applications. The role of disulfide linkages, electrostatic as well as hydrophobic interactions, in napin stability have been investigated through spectroscopic methods, employing different fluorescent probes and additives. The subunits are hydrophilic in nature and possess extended structure. With the addition of 0.5 M NaCl, the surface hydrophobicity of napin decreases, whereas the helical content increases by 25%. In the presence of NaCl, emission maximum shifts toward shorter wavelength and the Stern−Volmer constant decreases from 6.5 to 3.4 M^{-1}, indicating compaction of napin. Na_2SO_4 has no significant effect on the structure due to the lack of a hydrophobic core. In the presence of monohydric alcohols and trifluoroethanol, there is an increase in ordered structure. These studies indicate that the structure of napin, which is hydrophilic in nature, is stabilized by electrostatic interactions, in addition to disulfide linkages.

KEYWORDS: Mustard; napin; salt effect; monohydric alcohol; surface hydrophobicity

INTRODUCTION

Seed proteins can be classified into storage, structural, and biologically active proteins (*1*). The important storage proteins in mustard (*Brassica juncea* L.) seed are cruciferins and napins. Napins (2S albumins)—low molecular weight basic proteins—are rich in glutamine, lysine, and cysteine (*2*). Mustard has a well-balanced amino acid profile, compared to grains and legumes, which are deficient in sulfur-containing amino acids, and a favorable protein efficiency ratio of 2.6 in comparison with 2.2 for soybean (*3*). The functional potential of napins needs to be explored (*4*).

Allergenicity as well as resistance to trypsin limits the utilization of napins in food. One of the features of allergens is that the protein must have properties that protect its structure against degradation in the gastrointestinal tract. The 2S albumin family is highly stable to proteolysis as well as thermal denaturation. In the case of 2S albumin from Brazil nut, the intrachain disulfide bond pattern of the large subunit plays an important role in holding the core structure together against proteolysis (*5*).

Mustard napin consists of two subunits (of 29 and 86 residues) with two inter- and two intradisulfide bonds (*6*). There is a single tryptophan in the small subunit, whereas the large subunit has one tyrosine residue. Napin has potential as a flavor enhancer due to the high glutamine content (24%) in the protein (*7*). The secondary structure arrangement of napin reveals that these proteins are tightly packed in the seed (*8*). Thus, probing napin structure gains interest. Apart from disulfide linkages, hydrophobic and electrostatic interactions are the important parameters affecting protein structure.

Hydrophobic interactions play a major role in protein conformation (*9*). Hydrophobicity of proteins helps in understanding and predicting the effects of manipulation of protein sequence. There are limited reports on the hydrophobicity of mustard napin. We have calculated surface hydrophobicity of napin using aliphatic and aromatic fluorescent probes. The increase in the fluorescence emission intensity upon binding to accessible hydrophobic surface regions of proteins is used as a measure in the calculation of surface hydrophobicity. ANS, TNS, and CPA are charged probes, whereas PRODAN is a neutral probe used to eliminate the contribution of electrostatic interactions during fluorescence measurements (*10*). Organic solvents such as monohydric alcohols induce more ordered helical conformation relative to the native state of the protein (*11*). The addition of alcohols to the protein solution, apart from inducing α-helix structures, favors clustering of hydrophobic groups and better compactness in proteins (*12*, *13*). We have used NaCl, Na_2SO_4, monohydric alcohols, and TFE to explore the underlying forces that stabilize the napin molecule.

MATERIALS AND METHODS

Sephadex G-50 and CM-Sephadex were from Pharmacia Fine Chemicals, Uppsala, Sweden. 8-Anilino-1-naphthalene sulfonic acid

* Author to whom correspondence should be addressed (telephone +91 821 2515331; fax +91 821 2517233; e-mail appurao@cftri.res.in).

10.1021/jf0700935 CCC: $37.00
Published on Web 04/17/2007

(ANS) was from Aldrich Chemical Co., Milwaukee, WI. Dithiothreitol, iodoacetamide, acrylamide, bisacrylamide, sodium dodecyl sulfate, tris base, TNS, and urea were from Sigma Chemical Co., St. Louis, MO. A standard low molecular weight electrophoresis marker kit was from Genei, Bangalore, India. *cis*-Parinaric acid and PRODAN were from Molecular Probes Inc., Eugene, OR. Ampholine PAGplate and isoelectric focusing standards of broad p*I* (3.5−9.3) were from Amersham Biosciences, Little Chalfont, U.K. All other chemicals were of analytical grade. All protein purification experiments were carried out in 0.02 M phosphate buffer, pH 7.0 (buffer A).

Purification of Low Molecular Weight Napin (Protein) from *B. juncea*. Napin was purified according to a method reported earlier with modifications (*14*). Briefly, defatted mustard seeds were ground before being extracted with 1 M NaCl (1:10 w/v). The suspension was centrifuged, and ammonium sulfate was added (15−40%) to the supernatant. The pellet, after centrifugation, was dialyzed and loaded onto a Sephadex G-50 (1.5 × 200 cm, 350 mL) pre-equilibrated with buffer A containing 0.1 M NaCl. Protein peaks corresponding to napin were pooled (170−185 mL). Pooled samples were fractionated on a CM-Sephadex column (2.1 × 7 cm, 25 mL); bound protein was eluted with buffer (using a linear gradient of 0−0.5 M NaCl in buffer A) at a flow rate of 10 mL/h.

Homogeneity was ascertained by nonreducing 15% SDS-PAGE (*15*). Protein concentration was determined by using an $E^{1\%}_{1cm}$ value of 4.8. Gel filtration was carried out on a Waters HPLC system equipped with binary pump and photodiode array detector using a TSK-2000 gel filtration column pre-equilibrated with buffer A. The elution of the sample was carried out isocratically with flow rate maintained at 0.2 mL/min at 25 °C.

Amino-Terminal Sequencing. The peak fraction of purified napin was analyzed for amino-terminal sequencing on an Applied Biosystems Procise 4.0 instrument. The reduced subunits were blotted onto polyvinyl difluoride membrane after SDS-PAGE. Electrophoretic transfer (mini Trans-Blot) was carried out in 0.01 M CAPS buffer (pH 10.5) with 10% methanol (v/v) (100 V, 4 h at 25 °C). The membranes were stained with Ponceau stain to identify the subunits. The excised band was subjected to N-terminal sequencing by automated Edman degradation.

Isoelectric Focusing. Isoelectric focusing of the napin was performed at 10 °C on an Amersham Biosciences Multiphor-II apparatus. Ampholine PAGplate, a polyacrylamide gel, with a pH range of 3.5−9.5, was used. A broad p*I* kit (3.5−9.3) was used as standard. Protein (3 mg/mL) and markers were loaded directly onto the gel with sample application pieces (*16*).

Intrinsic Fluorescence Measurements. Fluorescence measurements were performed using a Shimadzu RF-5000 spectrofluorometer. The protein was excited at 280 nm, and the emission spectra were recorded in the region of 300−400 nm with excitation and emission slit widths set at 5 and 10 nm, respectively. The temperature of the cell was maintained at 27 °C by a circulating water bath (Huber, Offenburg, Germany). Fluorescence measurements were carried out using a 10 mm path length cell. The intrinsic fluorescence, in the presence of NaCl, KCl, and Na_2SO_4, was measured after the incubation of napin with the respective salt for 30 min.

Conformational Studies Using Proteolytic Enzymes. Conformational studies were carried out using TPCK-treated α-trypsin. Napin was digested with trypsin using an enzyme to substrate ratio of 2:100. The digestion was performed in 0.05 M ammonium bicarbonate buffer (pH 8.1) at 37 °C. Samples were drawn at regular intervals of 15 min, and the degree of hydrolysis was estimated by using the TNBS method (*17*). The hydrolytic behavior of trypsin on napin was also monitored by SDS-PAGE and RP-HPLC. The amino-terminal sequence of the purified peptide was carried out on an Applied Biosystems Procise 4.0 instrument. The molecular weight of the peptide was analyzed by MALDI-TOF.

Separation of Subunits. The large and small subunits were separated according to reported procedures (*8*) with a little modification. Napin was denatured with 8.0 M urea for 30 min and reduced by 0.1 M dithiothreitol at 27 °C for 2 h. Free cysteines were blocked using 0.2 M iodoacetamide in the dark for an hour. Subunits were separated on a G-50 Sephadex gel filtration column (140 × 0.5 cm, 110 mL). The purity of the two separated peaks (elution volumes of 40−48 and 60−66 mL) was ascertained by 17% SDS-PAGE and gel filtration on HPLC. Further structural characterization of separated subunits was carried out by absorption, fluorescence, and CD spectroscopy.

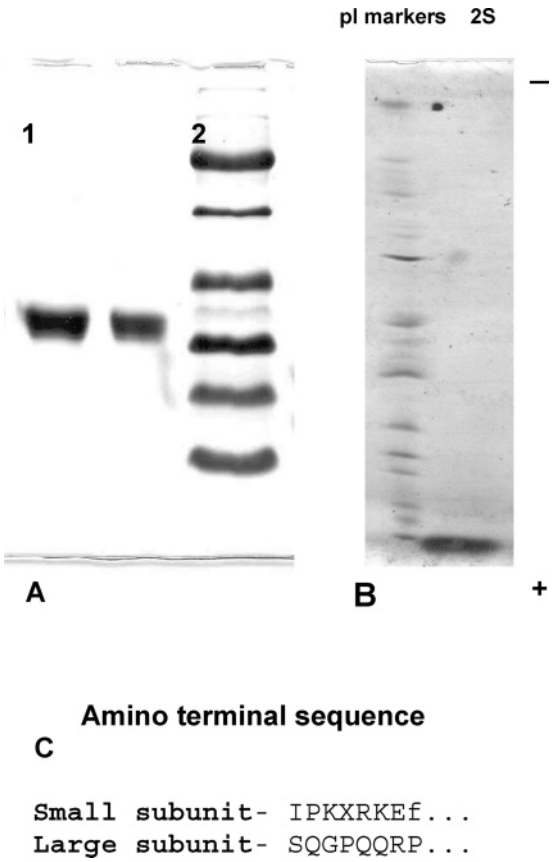

Figure 1. Establishing the homogeneity of *Brassica juncea* napin. (**A**) SDS-PAGE pattern under nonreducing condition (lane 1). The gel (15%) was stained with Coomassie brilliant blue R-250. Molecular weight markers in the range of 36000–3500 were run along with the protein (lane 2). The concentration of protein loaded was 1 mg/mL. (**B**) Isoelectric focused gel of napin. A concentration of 50 μg of napin was used for the experiment. The samples are loaded along with the standard p*I* markers. (**C**) Amino terminal sequence of large and small subunits of napin.

Hydropathy Plot. A hydropathy plot was constructed according to the method of Kyte and Doolittle (*18*). The plot was constructed using the available amino acid sequence (*B. juncea* CAA46785). Scores assigned for the most hydrophobic and for most hydrophilic amino acid were +4.5 and −4.5, respectively.

Surface Hydrophobicity Measurements. Napin surface hydrophobicity was measured using ANS, TNS, CPA, and PRODAN. Hydrophobicity was calculated according to the method of Cardamone and Puri (*19*). The binding constants were determined using a Scatchard plot. A stock solution of ANS ($\epsilon_{350} = 4.95 \times 10^3\ M^{-1}\ cm^{-1}$) (*19*) and TNS ($\epsilon_{366} = 4.3 \times 10^3\ M^{-1}\ cm^{-1}$) (*20*) was prepared in buffer A, whereas CPA ($\epsilon_{303} = 7.6 \times 10^4\ M^{-1}\ cm^{-1}$) and PRODAN ($\epsilon_{360} = 1.8 \times 10^4\ M^{-1}\ cm^{-1}$) were prepared in ethanol and methanol (analytical grade), respectively. For CPA, 10 μg of butylated hydroxyanisole (BHA) was added per milliliter of ethanol, to prevent oxidation. The stock solution was transferred into a brown bottle and stored at 4 °C (*10*). All reagents were prepared fresh.

Excitation wavelengths were 375, 366, 325, and 365 nm for ANS, TNS, CPA, and PRODAN, respectively. The emission spectra were collected from 400 to 500 nm using a 1 cm path length cell. The excitation and emission slit widths were 5 and 5 nm, respectively. Appropriate blanks in the corresponding solvents were subtracted to obtain the fluorescence enhancement caused by the fluorescent probe. Binding constants for the above ligands with napin were also determined

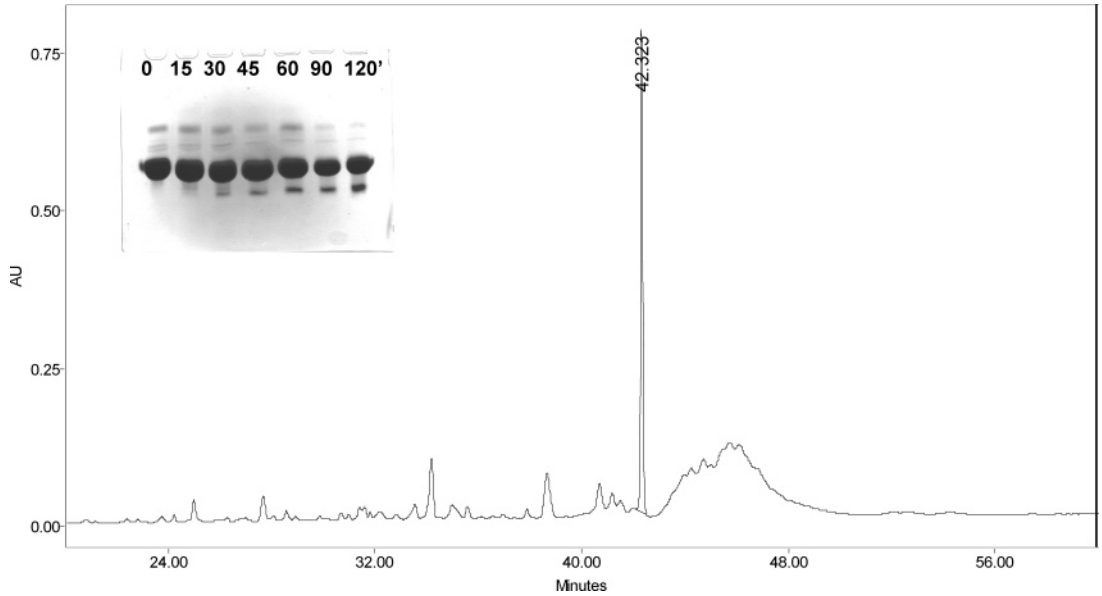

Figure 2. Trypsin digestion of napin; purification of tryptic digests on RP-HPLC. RP-HPLC was carried out using a symmetry shield C_{18} (5.0 μm, 4.6 mm $\times$ 250 mm) Waters column. Solvent A (0.1% TFA in water) and solvent B (100% acetonitrile containing 0.1% TFA) were used for gradient elution. The column was washed with solvent A for 10 min. Protein sample (20 μL) containing 20 μg was injected at a flow rate of 1 mL/min. The bound protein was eluted by a shallow gradient of acetonitrile from 0 to 50% over 70.0 min. The eluted protein was monitored at 230 and 280 nm. (Inset) Napin (4.0 mg/mL) was digested with α-TPCK-treated trypsin at 2:100 enzyme to protein ratio in 0.1 M ammonium hydrogen carbonate buffer (pH 8.2) at 37 °C. At different time intervals (0–120 min), aliquots were drawn, and digestion was terminated by adding 10 μM TLCK. The samples were analyzed by 15% nonreducing SDS-PAGE. The extent of hydrolysis was measured by using the TNBS method (*17*).

in the presence of NaCl and Na_2SO_4. The association constant was calculated using a Scatchard plot.

Fluorescence Quenching Measurements. To determine the exposure of tryptophan to solvent, fluorescence quenching measurements were done with the progressive addition of dynamic quencher (acrylamide) in the absence or presence of 0.5 M NaCl and 0.2 M Na_2SO_4. Protein solutions were centrifuged at 10000 rpm for 30 min before the scans. Titrations were carried out with excitation and emission slit widths of 5 and 10 nm, respectively. Napin concentration was fixed at 0.12 mg/mL.

The absorption of acrylamide at 280 nm was corrected using the Lehrer and Leavis equation. From the recorded titration spectra, the accessibility of tryptophan was calculated using the Stern−Volmer equation (*21*), namely

$$(F_0/F) - 1 = K_{SV}[Q]$$

where F_0 and F are the fluorescence intensities in the absence and presence of quencher, respectively, and K_{SV} is the Stern−Volmer constant.

Circular Dichroism (CD) Measurements. CD measurements were performed with a Jasco-810 automatic recording spectropolarimeter calibrated with *d*-(+)-10-camphor sulfonic acid. Dry nitrogen was purged continuously into the instrument before and during the experiment. The light path length of the cell used was 1 mm in the far-UV region (260−190 nm) and 10 mm in the near-UV region (320−240 nm). All measurements were made at 27 °C, and the mean residue ellipticity was calculated using a value of 110. The average of three scans at a speed of 10 nm/min, with a bandwidth of 1 nm and a response time of 1 s, was recorded. Protein concentrations of 0.4 and 2.5 mg/mL were used for far- and near-UV measurements, respectively. The effect of sodium chloride (0−1 M) or sodium sulfate (0−0.2 M) on the secondary and tertiary structure of napin was determined after incubation of the protein in salt for a period of 30 min. Changes in the secondary structure of napin, upon interaction with different concentrations of monohydric alcohols (methanol, ethanol, propanol, and butanol), were followed in the range of 2−18 M (alcohol concentration), at 222 nm. The studies were also made in the presence of 3−12 M trifluoroethanol (TFE).

Gel Filtration Chromatography. Gel filtration was carried out on a Bio-Gel P-30 column (0.6 $\times$ 35 cm) with a flow rate of 4.0 mL/h. The column was calibrated with marker proteins having known Stokes radii (R_S). Blue dextran (1 mg/mL) was used for determining the void volume (void volume, V_0 = 12 mL). The protein sample (4.0 mg/mL) was centrifuged at 10 °C and 10000 rpm for 20 min before it was loaded onto the column pre-equilibrated with buffer A. The experiment was repeated in the presence of 0.5 M NaCl and 0.2 M Na_2SO_4. The column was equilibrated with the required salt concentration in buffer A for the above.

Thermal Stability. The thermal stability of napin, in the presence or absence of 0.5 M NaCl, was followed by CD. The change in secondary structure, as a function of temperature, was monitored at 222 nm. Protein was heated in the temperature range of 27−75 °C at 1 °C/min using a peltier attachment (PMH 356WI). Protein concentration used for the study was 0.4 mg/mL in buffer A.

All results reported are the average of at least three determinations, unless otherwise mentioned.

RESULTS

Purification of Napin from *B. juncea*. Mustard napin was purified as reported earlier (*14*). Napin was precipitated with ammonium sulfate followed by gel filtration on Sephadex G-50 superfine. The peak corresponding to napin was pooled and loaded onto a CM-Sephadex ion exchange column and eluted with a 0−0.5 M NaCl gradient in buffer A. Napin eluted at 0.32 M NaCl. Homogeneity of the protein was ascertained by nonreducing 15% SDS-PAGE (**Figure 1A**) and gel filtration on HPLC (data not shown). The p*I* (isoelectric point) of napin was determined at pH >10.5 (shown in **Figure 1B**). The N-terminal sequence of reduced napin (**Figure 1C**) was similar to the deduced amino acid sequence from *B. juncea* napin (*6*).

Limited Proteolysis. Limited proteolysis of napin was carried out, using trypsin as a tool, to study the exposure of basic amino acid residues. The release of peptides as a function of time is shown in the inset of **Figure 2**. Digestion of napin by trypsin was feeble after 3−4 h of digestion. The protein digest, after

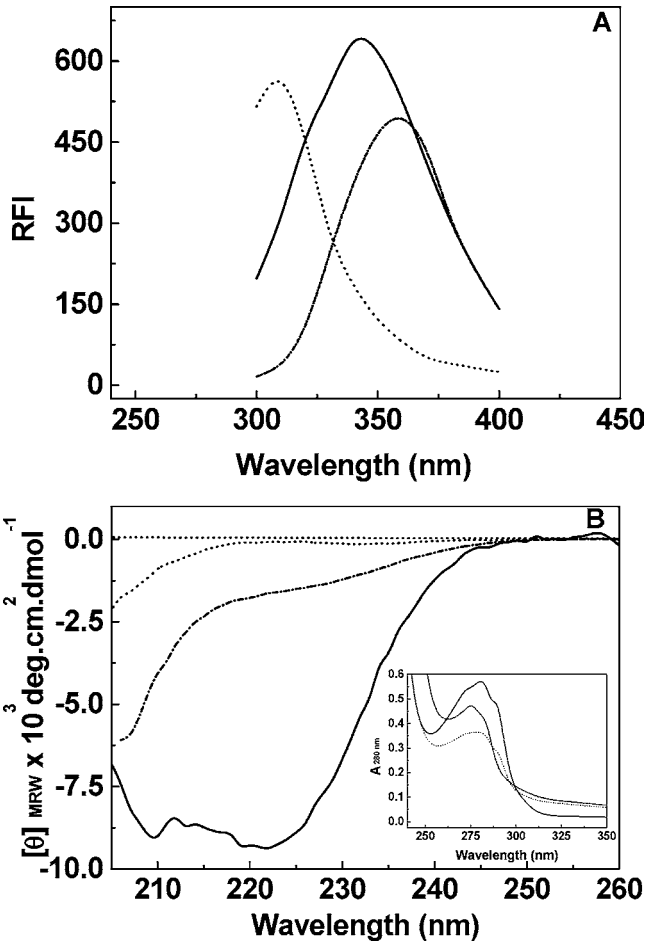

Figure 3. Characterization of separated subunits of *Brassica juncea* napin: (—) napin; (•••) small subunit; (–•–) large subunit in buffer A. (**A**) Fluorescence emission spectra. The emission spectra were recorded from 300 to 400 nm, when excited at 280 nm. The excitation and emission slit widths were at 5 nm. (**B**) Far-UV CD of napin and separated subunits. (Inset) Absorption spectra of napin and separated subunits recorded with 1 cm path length cell.

RP-HPLC, showed a major peptide peak at a retention time of 42 min (**Figure 2**). The molecular mass of the peptide was determined as ~6589 Da by MALDI-TOF. The peptide was found to be rich in cysteines and glutamines as determined by amino acid composition.

Hydrophobicity of Napin. The hydrophilic/hydrophobic nature of napin was determined using a Kyte and Doolittle hydropathy plot (data not shown). The sequence of napin used for the plot was from the GenBank database (*Brassica juncea* CAA46785). The plot confirmed the hydrophilic nature of napin.

Conformational Analysis of Napin. Napin contains a single tryptophan and tyrosine in its small and large subunits, respectively. The emission maximum is at 343 nm, suggesting the exposed nature of tryptophan in napin. The far-UV CD of napin has revealed two minima at 208 and 222 nm. The intact protein is rich in α-helix (~40%).

The contribution of subunits to the conformation of napin was studied by the reduction of disulfides and blocking the free thiol with iodoacetamide. The elution profile revealed two peaks, and the purity of the subunits was ascertained by 15% SDS-PAGE. Intrinsic fluorescence showed emission maxima of 353 and 305 nm, for small and large subunits, respectively (**Figure 3A**). This indicated the presence of tryptophan and tyrosine in small and large subunits, respectively. The two separated subunits were also hydrophilic in nature and devoid of buried hydrophobic patches. The absorption spectra of napin and separated subunits are shown as the inset of **Figure 3B**. Secondary structures of the subunits revealed only aperiodic structure (**Figure 3B**).

To understand the interactions responsible for the stability of napin, the effect of additives on the conformation of the protein was studied. The changes in surface hydrophobicity of napin were followed by fluorescent probes ANS, TNS, PRODAN, and CPA. To understand the effect of electrostatic and hydrophobic interactions, sodium chloride and sodium sulfate (0−1 M) were used. The effects of TFE, the helix promoter, and monohydric alcohols on the conformation of napin were followed.

Surface Hydrophobicity Measurements through Fluorescent Probes. Surface hydrophobicity can be classified into aliphatic and aromatic hydrophobicity. CPA is useful for determining the aliphatic hydrophobicity, because it is composed of aliphatic hydrocarbons and is a plant-derived 18-carbon fatty acid. ANS, due to its aromatic structure, is used for determining aromatic hydrophobicity (*22*). TNS, a derivative of ANS, although nonfluorescent, fluoresces when bound to hydrophobic regions of protein and can be used as a surface hydrophobic probe (*20*). On the other hand, PRODAN is a neutral probe, which eliminates electrostatic contribution in the measurement of hydrophobicity.

Plots of fluorescence quenching, upon progressive addition of ANS, TNS, PRODAN, and CPA, are shown in **Figure 4**. The Scatchard plots are given as insets. Binding constants and number of binding sites for the protein in the presence or absence of 0.5 M NaCl and 0.2 M Na_2SO_4 have been calculated and are shown in **Table 1**; 0.5 mol of fluorescent probe bound per mole of protein, indicating the hydrophilicity of napin. There is a reduction in binding constant and number of binding sites in the presence of NaCl as compared to control. The binding constant of CPA to napin is lower compared to the aromatic hydrophobic probes.

Effect of Salts on Napin Structure. *Fluorescence Measurements.* The effect of salts on the tertiary structure has been studied by fluorescence emission spectra. Napin, in buffer A, was incubated with different concentrations of KCl, NaCl, and Na_2SO_4 for 30 min. The relative fluorescence intensity increases with increasing salt concentration, and the emission maxima shifts toward blue (−4 nm for NaCl and −1 nm for Na_2SO_4). The effect of KCl on napin is found to be similar to that of NaCl. Beyond 0.5 M NaCl, the fluorescence intensity remains constant, whereas above 0.7 M, a decrease in intensity is observed. In the case of 0.2 M Na_2SO_4, the maximum increase in the fluorescence intensity has been observed at 0.2 M (**Figure 5A**, inset). Salt concentrations of 0.5 M NaCl and 0.2 M Na_2SO_4 were used for further measurements. A blue shift in the emission maximum, in the presence of salt, may be due to the environment around the tryptophan residue being more hydrophobic compared to native (**Figure 5A**).

Circular Dichroism Measurements. Changes in the secondary structure of napin, upon salt addition, were followed by far- and near-UV CD spectra. The ellipticity value increased up to ~25% in the presence of 0.5 M NaCl and 3% in the presence of Na_2SO_4. Beyond 1 M NaCl and 0.5 M Na_2SO_4, the ellipticity value (at 222 nm) decreased. In the presence of 0.5 M NaCl, the ellipticity ratio, R ($[\theta]_{222}/[\theta]_{208}$) increased from 1.05 to 1.25 ± 0.05, indicating a stronger interhelical association (**Figure 5B**) (*23*). In the presence of Na_2SO_4, the ratio was 1.07, indicating little or no change. The tertiary structure changes of

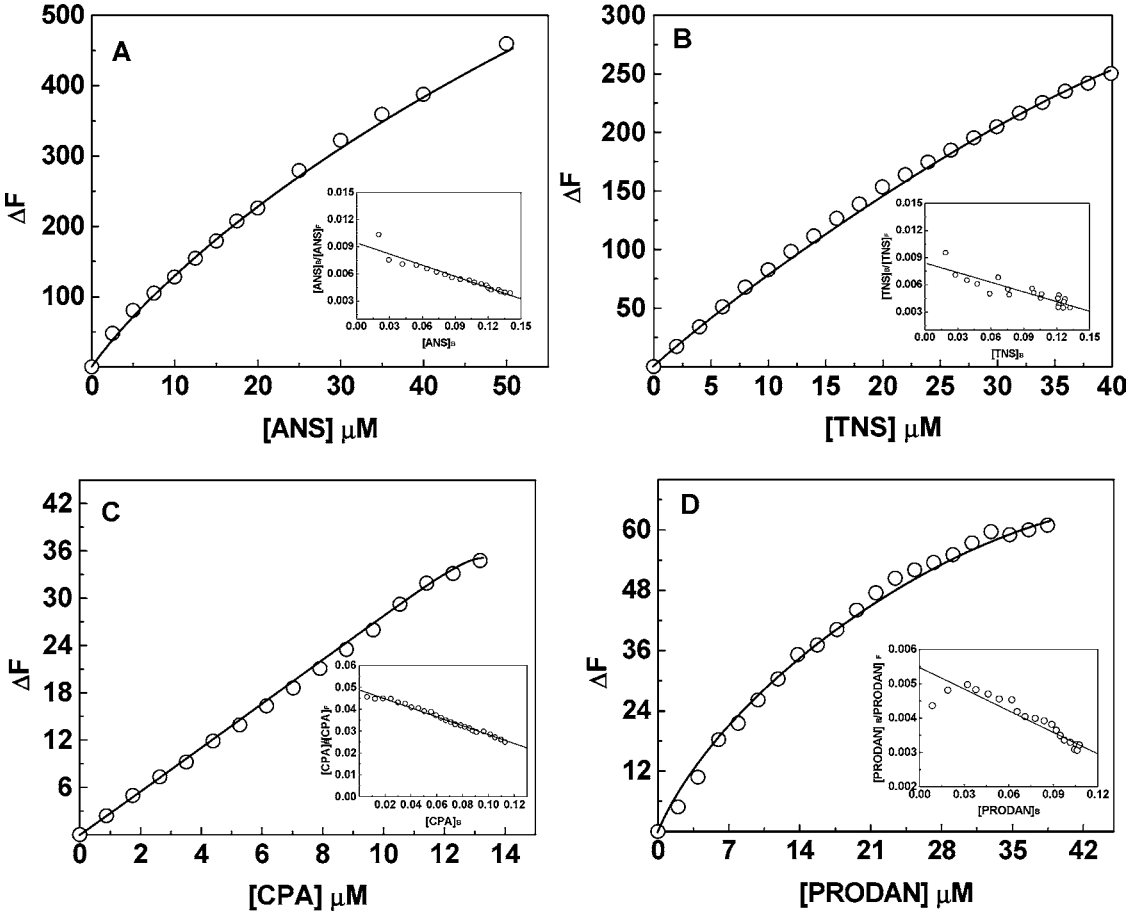

Figure 4. Surface hydrophobicity measurement of *Brassica juncea* napin; plot of increase in the (**A**) ANS–protein-bound fluorescence (emission followed at 480 nm when excited at 375 nm), (**B**) TNS–protein complex (emission at 460 nm when excited at 366 nm), (**C**) CPA–protein complex (emission at 420 nm when excited at 325 nm), and (**D**) PRODAN–protein complex (emission at 465 nm when excited at 365 nm). (Inset) Scatchard plots for determining the binding constants. The excitation and emission slit widths were 5 and 5 nm. Protein concentration used was 0.75 mg/mL.

Table 1. Binding Constants of Napin with Different Fluoroscent Probes[a]

control	ANS[b]	PRODAN[c]	TNS[d]	CPA[e]
no. of binding sites	0.48 ± 0.1	0.6 0.1	0.53 ± 0.1	0.6 ± 0.1
binding constant (M^{-1})	4.1×10^4	9.5×10^4	2.0×10^4	0.91×10^4
0.5 M NaCl				
no. of binding sites	0.21 ± 0.1	0.26 ± 0.1	0.3 ± 0.12	0.24 ± 0.1
binding constant (M^{-1})	2.1×10^4	4.3×10^4	1.19×10^4	0.46×10^4
0.2 M Na_2SO_4				
no. of binding sites	0.5 ± 0.1	0.45 ± 0.1	0.62 ± 0.1	0.52 ± 0.1
binding constant (M^{-1})	3.55×10^4	8.5×10^4	1.9×10^4	0.89×10^4

[a] A protein concentration of 0.75 mg/mL was used for all measurements. The results are average of three individual experiments. [b] Emission maximum of napin in presence of ANS was 480 nm when excited at 375 nm. [c] Emission maximum of napin in presence of PRODON was 465 nm when excited at 365 nm. [d] Emission maximum of napin in presence of TNS was 460 nm when excited at 366 nm. [e] Emission maximum of napin in presence of CPA was 420 nm when excited at 325 nm.

napin, in the presence of salts, were followed by near-UV CD, which showed no significant change in the ellipticity values at 0.5 M NaCl and 0.2 M Na_2SO_4 (**Figure 5C**).

Acrylamide Quenching of Intrinsic Fluorescence. Quenching of napin fluorescence by acrylamide, a nonionic quencher, is shown in **Figure 6A**. The Stern−Volmer plot has been used to obtain the constant, K_{SV} (**Figure 6B**). The fractional accessibility of the lone tryptophan, indicative of its exposure to solvent, is 0.63 (**Table 2**). In the presence of 0.5 M NaCl, the fractional accessibility is found to decrease to 0.5 and in the presence of sulfate remains at 0.6. The decrease in the K_{SV}, in the presence of NaCl, may be due to compaction of the molecule.

Table 2. Intrinsic Fluorescence Quenching by Acrylamide[a]

	Stern–Volmer constant K_{SV} (M^{-1})	fractional accessibility
control	6.5 ± 1.1	0.63 ± 0.14
0.5 M NaCl	3.4 ± 0.55	0.50 ± 0.1
0.2 M Na_2SO_4	6.2 ± 0.96	0.59 ± 0.11

[a] A protein concentration of 0.12 mg/mL was used for all measurements. The results are average of three individual experiments.

Gel Filtration. Native napin eluted at 17 mL in buffer A. In the presence of 0.5 M NaCl, the elution volume shifted to 18.2 mL, indicating a reduction in the Stokes radius. There was no significant change in the elution volume in the presence of 0.2 M Na_2SO_4 (data not shown).

***T*$_M$.** The effect of 0.5 M NaCl and 0.2 M Na_2SO_4 on the secondary structure loss was studied at 222 nm, in the temperature range of 27−75 °C (**Figure 6A**, inset). In the presence of 0.5 M NaCl, the T_M (transition temperature) shifted from 74 to 88 °C, indicating increased protein stability.

Effect of Monohydric Alcohols on Napin Structure. Solvents play an important role in maintaining the native structure of a protein. Structural studies of proteins in the presence of different solvent systems can provide information on their unique folded structure in solution. The propensity to

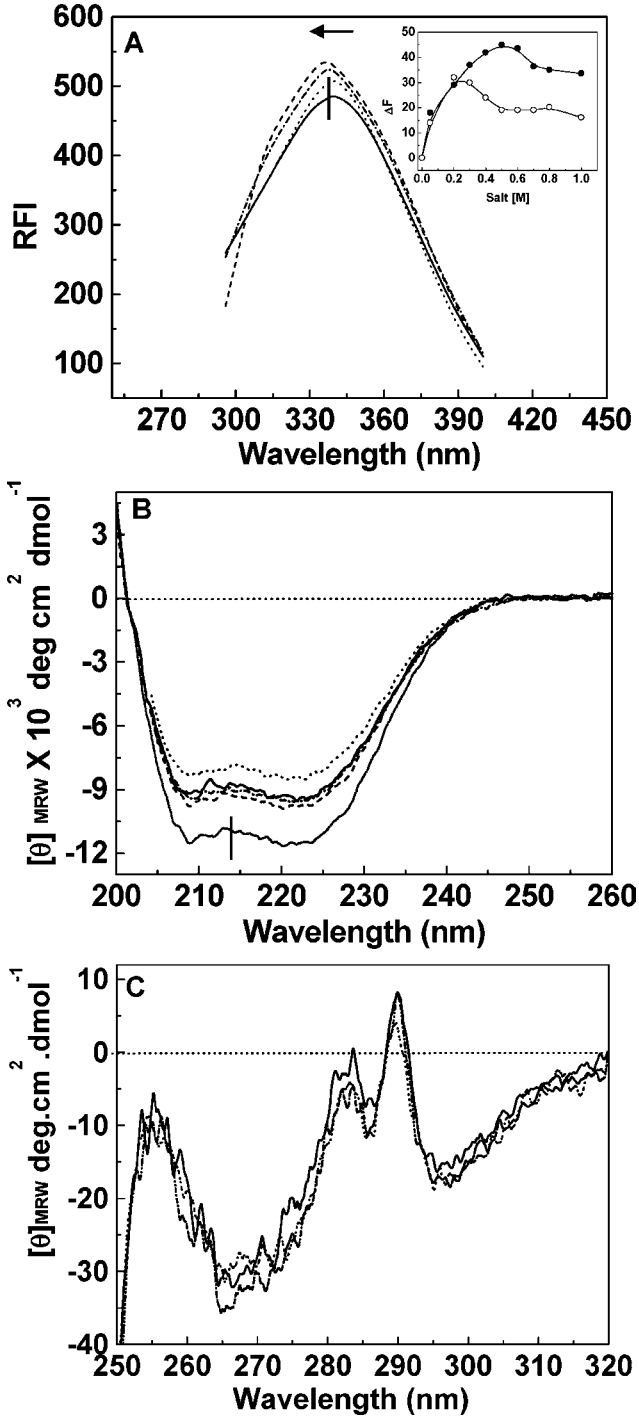

Figure 5. Salt-induced conformational changes in napin structure. (**A**) Changes in fluorescence emission intensity of (—) napin in buffer A, (•••) napin in 0.2 M NaCl, (- - -) napin in 0.5 M NaCl, and (–•–) napin in 0.75 M NaCl. (Inset) Plot of change in the relative fluorescence intensity as a function of (●) NaCl and (○) Na_2SO_4. (**B**) Far-UV CD spectra: (---) napin in buffer A; (••••) napin in 0.2 M Na_2SO_4; (—) napin in 0.5 M NaCl; (–•–) napin in 0.75 M NaCl; (–••–) napin in 1.0 NaCl. (**C**) Near-UV CD spectra: (—) napin in buffer; (•••) napin in 0.5 M NaCl; (- - -) napin in 0.2 M Na_2SO_4. Both near- and far-UV CD measurements were performed on a Jasco-J 810 automatic recording spectropolarimeter. The spectra were recorded at a scan speed of 20 nm/min. An average of at least three accumulations is shown. Mean residue weight of 110 was used to calculate the molar ellipticity. For far-UV scans (200–260 nm), protein (0.4 mg/mL) in buffer A was used. Protein concentration of 2.5 mg/mL was used in the near-UV region (320–240 nm). Path lengths of the cells were 1 and 10 mm for the far-UV and near-UV scans, respectively.

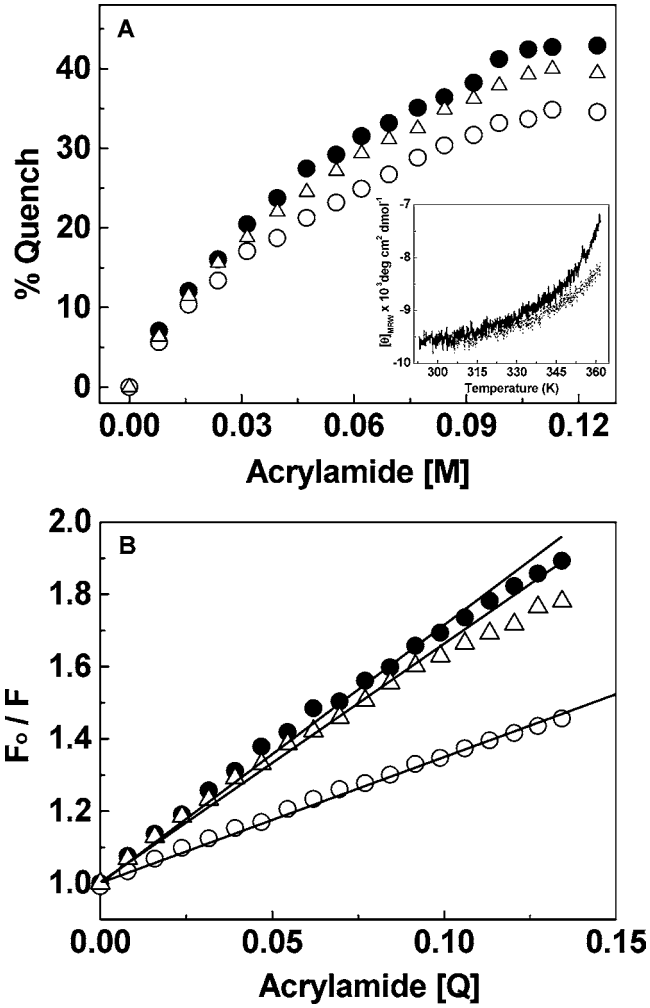

Figure 6. Intrinsic fluorescence quench of *Brassica juncea* napin by acrylamide. (**A**) Primary plot of fluorescence quench as a function of acrylamide concentration: (●) napin in buffer A; (○) napin in the presence of 0.5 M NaCl; (△) napin in 0.2 M Na_2SO_4. The accessibility of tryptophan was calculated using a modified Stern–Volmer equation. Protein concentration of 0.12 mg/mL was used for all measurements. Napin was excited at 280 nm, and the emission spectra were recorded in the region of 300–400 nm. Excitation and emission slit widths were set at 5 and 10 nm, respectively. (Inset) Temperature-induced unfolding of napin in the presence and absence of 0.5 M NaCl, monitored at 222 nm. The protein in buffer A was heated in the temperature range 27–75 °C, at a heating rate of 1 °C/min: (—) napin in buffer A; (•••) napin in 0.5 M NaCl. Mean residue weight of 110 was used to calculate the molar ellipticity. Protein (0.4 mg/mL) in buffer A was used for the measurements. (**B**) Stern–Volmer plot for acrylamide-quenched fluorescence of napin: (●) napin in buffer A; (○) napin in the presence of 0.5 M NaCl; (△) napin in 0.2 M Na_2SO_4.

form α-helix (38%) reached a maximum at 17 M methanol concentration, beyond which the protein precipitated. Napin, in the presence of 8.25 M ethanol, showed a 28% increase in α-helix. Above a 15 M ethanol concentration, protein precipitated. Similar studies, in the presence of propanol and butanol, revealed an increase in α-helix (20% increase in propanol and 10% increase with butanol) at 6.7 and 3.5 M concentrations, respectively.

The effect of TFE (helix promoter) on the secondary structure is shown in **Figure 7**. The change in molar ellipticity as a function of TFE is shown in the inset of **Figure 7**. An increase

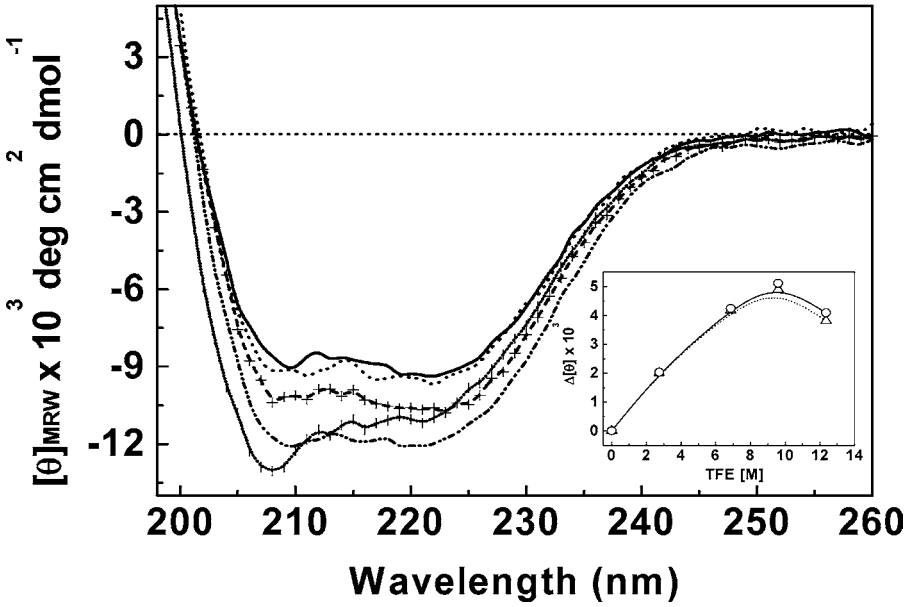

Figure 7. TFE-induced structural changes in napin. Far-UV CD specta: (—) napin in buffer A; napin in (•••) 3.0 M, (++) 6.0 M, (•••|•••) 10.0 M; or (–•–•–) 12.0 M TFE. Scans were recorded in the region of 200–260 nm using a 1 mm path length cell. Protein concentration was 0.4 mg/mL. The samples were centrifuged before the spectra were recorded. (Inset) Plot of the changes in the ellipticity at 222 nm as a function of TFE concentration.

in α-helix (50%) at 10 M TFE concentration was seen. Beyond 10 M TFE, protein precipitation was observed.

DISCUSSION

Napin from mustard (*B. juncea* L) is synthesized as a precursor protein and translocated into endoplasmic reticulum, where the intrachain disulfide bonds are formed. The proprotein is transported via a secretory pathway to the vacuole, where the negatively charged prosequences are proteolytically cleaved (*24*) to yield the mature napin. Napin is found to be antifungal and antimicrobial (*25*). Although mustard protein has a well-balanced amino acid profile and a favorable protein efficiency ratio, its utility as a food source of protein is limited by its allergenicity. We have investigated the contributions of the different interactions to the stability of napin.

In the present study, napin is purified and identified by comparing the amino-terminal sequence of two separated subunits to the available deduced amino acid sequence of *B. juncea* (*6*). The protein has ∼40% helix and is highly hydrophilic, as shown by the Kyte and Doolittle hydropathy plot. Napin is resistant to trypsin digestion. A peptide, rich in glutamine and cysteine, has been obtained at the end of 2 h, with most of the protein remaining intact (**Figure 2**). Napins from *Brassica* species are resistant to proteolysis by gastric enzymes (*26*).

Extrinsic fluorescence probes such as ANS, TNS, CPA, and PRODAN have been used for determining the aromatic and aliphatic (CPA) hydrophobicity of napin. The binding constants for all of the above probes are low (**Table 1**), with only ∼0.5 mol binding to 1 mol of protein. The binding constant decreases in the presence of 0.5 M NaCl concentration. These values confirm the hydrophilic nature of the molecule. No significant change in the surface hydrophobicity is observed in the presence of Na_2SO_4.

Addition of 0.5 M NaCl and 0.2 M Na_2SO_4 results in shifts of the emission maximum of 5 and 1 nm, respectively, toward shorter wavelength. The fractional accessibility of the single tryptophan in napin has been evaluated by following the quenching of intrinsic fluorescence by acrylamide in the absence and presence of 0.5 M NaCl. The Stern−Volmer constant decreases from 6.5 to 3.4 M^{-1}, indicating compactness in the presence of NaCl. The compaction of the molecule in the presence of 0.5 M NaCl is further confirmed by gel filtration.

Na_2SO_4 does not affect the secondary structure of napin. Addition of NaCl results in an increase of 25% helical structure as monitored by far-UV CD spectra. The changes in the thermal transition (T_M) and elution volume could be due to compaction of protein. On the basis of its sequence (GenBank CAA46785), napin has a net positive charge of +9 at neutral pH. Hence, it is likely that the anions play a key role in the salt effect on napin. The high net positive charge coupled with low hydrophobicity suggests that napin is a rather weakly folded protein driven largely by disulfide linkages. Charge neutralization or preferential exclusion (of the salt) from the vicinity of the protein results in compactness in the presence of high salt concentrations (*27*, *28*).

The propensity for napin to form structure, in the presence of intramolecular interaction enhancing organic solvents such as alcohols and TFE, has been studied. Monohydric alcohols and TFE induce structure as evidenced by increased helical content of napin. TFE is known to be an intramolecular hydrogen bond enhancer and protects solvent-exposed hydrophobic residues from aggregating. Low concentrations of monohydric alcohols on napin show the propensity to form α-helix in the presence of alcohols in the order TFE > methanol > ethanol > propanol > butanol.

The structural changes induced by alcohols are reversible. Higher concentrations of propanol (>6.7 M) and butanol (>3.5 M) result in protein precipitation. Recent studies have shown that at low concentrations, TFE and monohydric alcohols act by a cosmotropic mechanism to promote desolvation of the polypeptide backbone and not directly through stabilization of helical structures or strengthening hydrogen bonds (*29*).

Our results can be summarized as follows:

(1) Na_2SO_4 does not affect napin structure or stability due to the absence of a hydrophobic core. Addition of NaCl results in compaction of mustard napin, thereby stabilizing it.

(2) Electrostatic interactions play a major role in stabilizing the protein structure in addition to the presence of disulfide linkages.

The compaction of napin in the presence of salts may increase our understanding of the digestibility and allergenicity of the molecule.

ABBREVIATIONS USED

T_M, transition temperature; CD, circular dichroism; PVDF, polyvinyl difluoride; TNBS, trinitrobenzene sulfonic acid; ANS, 8-aniline naphthalene sulfonic acid; PRODAN, 6-propionyl-2-(*N*,*N*-dimethylamino)naphthalene; CPA, *cis*-parinaric acid; TNS, 2-*p*-toluidinylnaphthalene-6-sulfonate; TFE, trifluoroethanol.

ACKNOWLEDGMENT

We thank Dr. V. Prakash, Director, CFTRI, for his suggestions and providing facilities. We thank P. S. Kulashekar for help in preparation of the manuscript and Dr. Lalitha R. Gowda for rendering help in amino-terminal sequencing.

LITERATURE CITED

(1) Mandal, S.; Kundu, P.; Roy, B.; Mandal, R. K. Precursor of the inactive 2S protein from the Indian mustard *Brassica juncea* is a novel trypsin inhibitar. *J. Biol. Chem.* **2002**, *277*, 37161−37168.

(2) Schmidt, I.; Renard, D.; Rondeau, D.; Richomme, P.; Viguier Axelos, M. A. Detailed physicochemical characterization of the 2S storage protein from rape (*Brassica napus* L.). *J. Agric. Food Chem.* **2004**, *52*, 5995−6001.

(3) Delisle, J.; Amiot, J.; Goulet, G.; Simard, C.; Brisson, G.; Jones, J. Nutritive value of protein fractions extracted from soybean, rapessed and wheat flours in the rat. *Qual. Plant Foods Hum. Nutr*. **1984**, *34*, 243−251.

(4) Barciszewski, J.; Szymanski, M.; Haertle, T. Minireview: analysis of rapeseed napin structure and potential roles of the storage protein. *J. Protein Chem.* **2000**, *19*, 249−254.

(5) Moreno, F. J.; Mellon, F. A.; Wickham, M. S. J.; Bottrill, A. R.; Clare Mills, E. N. Stability of the major allergen brazil nu t 2S albumin (Ber e 1) to physiologically relevant *in vitro* gastrointestinal digestion. *FEBS J.* **2005**, *272*, 341−352.

(6) Dasgupta, J.; Dasgupta, S.; Ghosh, S.; Roy, B.; Mandal, R, K. Deduced amino acid sequence of 2S storage protein from *Brassica* species and their structural features. *Indian J. Biochem. Biophys.* **1995**, *32*, 378−384.

(7) Halpern, B. P. Glutamate and the flavor of foods. *J. Nutr*. **2000**, *130*, 910S−914S.

(8) Menendez-Arias, L.; Monsalve, R. I.; Gavilanes, J. G.; Rodriguez, R. Molecular and spectroscopic characterization of a low molecular weight seed storage protein from yellow mustard (*Sinapis alba*). *Int. J. Biochem*. **1987**, *19*, 899−907.

(9) Privalov, P. L.; Gill, S. J. Stability of protein structure and hydrophobic interaction. *Adv. Protein Chem.* **1988**, *39*, 191−234.

(10) Alizadeh-Pasdar, N.; Li-Chan, E. Comparison of protein surface hydrophobicity measured at various pH values using three different fluorescent probes. *J. Agric. Food. Chem*. **2000**, *48*, 328−334.

(11) Herskovits, T. T.; Gadegbeku, B.; Jaillet, H. On the structural stability and solvent denaturation of proteins. *J. Biol. Chem*. **1970**, *245*, 2588−2598.

(12) Arakawa, T.; Goddette, D. The mechanism of helical transition of proteins by organic solvents. *Arch. Biochem. Biophys.* **1985**, *240*, 21−32.

(13) Usha, R.; Maheshwari, R.; Dhathathreyan, A.; Ramasami, T. Structural influence of mono and polyhydric alcohols on the stabilization of collagen. *Colloids Surf. B: Biointerfaces* **2006**, *48*, 101−105.

(14) Venkatesh, A.; Rao, A. G. A. Isolation and characterization of low molecular weight protein from mustard (*Brassica juncea*). *J. Agric. Food Chem*. **1988**, *36*, 1150−1155.

(15) Laemmli, U. K. Cleavage of structural proteins during the assembly of the head of bacteriophage T4. *Nature* **1970**, *227*, 680−685.

(16) Jyothi, T. C.; Singh, S. A.; Rao, A. G. A. The contribution of ionic interactions to the conformational stability and function of polygalacturonase from *A. niger*. *Int. J. Biol. Macromol*. **2005**, *36*, 310−317.

(17) Nissen, J. A. Determination of degree of hydrolysis of food protein hydrolysates by trinitrobenzene sulfonic acid. *J. Agric. Food Chem.* **1979**, *27*, 1256−1262.

(18) Kyte, J.; Doolittle, R. A. simple method for displaying the hydropathic character of a protein. *J. Mol. Biol*. **1982**, *157*, 105−132.

(19) Cardamone, M.; Puri, N. K. Spectrofluorimetric assessment of the surface hydrophobicity of proteins. *Biochem. J*. **1992**, *282*, 589−593.

(20) McClure, W. O.; Edelman, G. M. Fluorescent probes for conformational states of proteins. The binding of 2-*p*-toluedinylnaphthalene-6-sulfanate to α-chymotrypsin. *Biochemistry* **1967**, *6*, 559−566.

(21) Eftink, M. R. In *Topics in Fluorescence Spectroscopy*, 2nd ed.; Lakowicz, J. R., Ed.; Plenum Press: New York, 1991; pp 53−102.

(22) Moro, A.; Gatti, C.; Delorenzi, N. Hydrophobicity of whey protein concentrates measured by fluorescence quenching and its relation with surface functional properties, *J. Agric. Food Chem.* **2001**, *49*, 4784−4789.

(23) Lazo, N. D.; Downing, D. T. Effects of Na_2SO_4 on hydrophobic and electrostatic interactions between amphipathic α-helices. *J. Pept. Res.* **2001**, *58*, 457−463.

(24) Muren, E.; Ek, B.; Bjork, I.; Rask, L. Structural comparison of the precursor and the mature form of napin, the 2S storage protein in *Brassica napus*. *Eur. J. Biochem.* **1996**, *242*, 214−219.

(25) Onaderra, M.; Monsalve, R. I.; Manchero, J. M.; Villalba, M.; Martinez del Pozo, A.; Gavilanes, J. G.; Rodriguez, R. Food mustard allergen interaction with phospholipid vesicles. *Eur. J. Biochem.* **1994**, *225*, 609−615.

(26) Pantoja-Uceda, D.; Palomares, O.; Bruix, M.; Villalba, M.; Rodríguez, R.; Rico, M.; Santoro, J. Solution structure and stability against digestion of rproBnIb, a recombinant 2S albumin from rapeseed: relationship to its allergenic properties. *Biochemistry* **2004**, *43*, 16036−16045.

(27) Gouda, M. D.; Singh, S. A.; Rao, A. G. A.; Thakur, M. S.; Karanth, N. G. Thermal inactivation of glucose oxidase: mechanism and stabilization using additives. *J. Biol. Chem.* **2003**, *278*, 24324−24333.

(28) Nishimura, C.; Uversky, V. N.; Fink, A. L. Effect of salts on the stability and folding of staphylococcal nuclease. *Biochemistry* **2001**, *40*, 2113−2128.

(29) Kentsis, A.; Sosnick, T. R. Trifluoroethanol promotes helix formation by destabilizing backbone exposure: desolvation rather than native hydrogen bonding defines the kinetic pathway of dimeric coiled coil folding. *Biochemistry* **1998**, *37*, 14613−14622.

Received for review January 12, 2007. Revised manuscript received March 14, 2007. Accepted March 22, 2007. T.C.J. thanks CSIR, India, for a Senior Research Fellowship.

JF0700935